ISSN 0036-0244, Russian Journal of Physical Chemistry A, 2022, Vol. 96, No. 3, pp. 502–507. © Pleiades Publishing, Ltd., 2022.

CHEMICAL THERMODYNAMICS AND THERMOCHEMISTRY

Calculation of Virial Coefficients, Joule–Thomson Inversion Curve and Mutual Diffusion for Binary Mixtures

Mohammad Almasi[a,*]

[a]*Department of Applied Chemistry, Faculty of Science, Malayer University, Malayer, 65174 Iran*

**e-mail: m.almasi@malayeru.ac.ir*

Received January 14, 2021; revised March 24, 2021; accepted March 25, 2021

Abstract—In this study, the reliability of the Peng–Robinson–Stryjek–Vera (PRSV) cubic equation of state to estimate the second and third virial coefficients and the Joule–Thomson inversion curves for the binary mixtures of benzene with 2-propanol, 2-butanol, and 2-pentanol was demonstrated. Besides, the mutual diffusion coefficients for the binary mixtures in the whole composition range were determined. Obtained results indicate that the considered mixtures show a positive deviation from Raoult's Law. The results were analyzed to gain information to understand the structure of liquid influencing the diffusion phenomenon. The interplay between kinetic and thermodynamic contributions on the mutual diffusion coefficients was discussed. It has been shown that the structural changes and intermolecular interactions between benzene and 2-alkanol, which changes with the alcohol chain length, have a significant impact on the diffusion process. The investigation has shown that increasing in the alcohol chain length reinforces the strength of intermolecular forces.

Keywords: virial coefficients, mutual diffusion, benzene, 2-alkanol

DOI: 10.1134/S0036024422030189

INTRODUCTION

Virial equations of state are functions that explain the $P–V–T$ behavior of pure materials or mixtures. In this equation, the compressibility factor Z is written in a power series in molar volume [1]:

$$Z = \frac{PV}{RT} = 1 + B\frac{1}{V} + C\frac{1}{V^2} + \dots . \quad (1)$$

The coefficients of this expansion (B, C...) named virial coefficients. Different experimental and theoretical methods are available to estimate the virial coefficients. Experimental techniques include PVT, relative permittivity, and speed of sound [2–5]. Theoretical approaches consist of using equations of state and interaction potential. Among these methods, equations of state (EOS) are highly suitable tools to calculate the virial coefficients. The virial coefficients are related to intermolecular forces. For instance, the second virial coefficient indicates the effect of the interaction between two molecules, and so on. From this perspective, the virial coefficients represent the nonideal behavior of real substances. Hence, accurate information about the virial coefficients is of considerable significance [6–9]. Careful screening of the literature indicates that no experimental virial coefficients for the mixtures studied are available.

The Joule–Thomson effect explains the temperature change of a gas or liquid when undergoes the pressure changes while the process is isenthalpic.

$$\mu = \left(\frac{\partial T}{\partial P}\right)_H . \quad (2)$$

The Joule–Thomson inversion curve (JTIC) [10–13] is a place in the $P–T$ plane where $\mu = 0$. JTIC calculation is one of the most required parameters for equations of state. PRSV EOS [14] is a powerful tool for calculation of the JTIC for the binary mixtures.

Diffusion coefficients are valuable and essential in industrial technology developments and academic researches. However, due to the strict required experimental condition, it is difficult to determine the diffusion data experimentally. Therefore, reliable theoretical studies or computer simulations are the essential methods to obtain diffusion coefficients of fluids.

This paper is conducted as follows. First, using the PRSV equation of state to predict the second and third virial coefficients for the binary mixtures of benzene with 2-propanol, 2-butanol, and 2-pentanol. Second, the JTIC for the above binary mixtures was determined regarding the PRSV EOS. Subsequently, the mutual diffusion coefficients were calculated for the above binary liquid mixtures over the whole concentration range at 303.15 K. The current study continues our efforts [15–39] to detailed study of molecular forces in the solutions containing alkanols.

THEORY

Equation of State

Prediction of the virial coefficient of pure substances and fluid mixtures is one of the essential applications of equations of state. In the virial expansion, the compressibility factor expressed as a power series in density or reciprocal volume. The general expression for PRSV equation of state is as follows [14]

$$P = \frac{RT}{V-b} - \frac{a(T)}{(V^2+2bV-b^2)} \tag{3}$$

with

$$a = (0.457325R^2T^2/P_c)\alpha, \tag{4}$$

$$\alpha = [1+\kappa(1-T_R^{0.5})]^2, \tag{5}$$

$$b = 0.077796RT_c/P_c. \tag{6}$$

The κ term has the form

$$\kappa = \kappa_0 + \kappa_1(1-T_R^{0.5})(0.7-T_R), \tag{7}$$

$$\kappa_0 = 0.378893 + 1.489715\omega - 0.1713848\omega^2 + 0.0196544\omega^3, \tag{8}$$

κ_1 is an adjustable parameter for the pure compounds and ω is the acentric factor. Values of κ_1 parameter for the pure materials were taken from [14, 40], while for 2-pentanol was obtained with the correlation method (0.3827). The applied mixing rules for binary mixtures are as follow:

$$a = \sum_i \sum_j x_i x_j (a_i a_j)^{0.5}(1-k_{ij}), \tag{9}$$

$$b = \sum_i \sum_j x_i x_j \left(\frac{b_i+b_j}{2}\right), \tag{10}$$

k_{ij} is an adjustable parameter. The ith virial coefficient (c_i) could be obtained as [41]

$$c_i = \frac{\lim\limits_{\rho\to 0}\left(\frac{\partial Z^{i-1}}{\partial^{i-1}\rho}\right)}{(i-1)}. \tag{11}$$

The Joule–Thomson Inversion Curve (JTIC)

Equation (2) is expressed in an alternative frame as [1]:

$$dH = Tds + VdP. \tag{12}$$

After derivation of the above equation to P, using the Maxwell relationship and some simplifications, we have

$$\mu = \frac{1}{c_p}\left[T\left(\frac{\partial V}{\partial T}\right) - V\right]. \tag{13}$$

At the inversion temperature, $\mu = 0$ and the most frequent form of the JTIC is [10]

$$T\left(\frac{\partial P}{\partial T}\right)_V + V\left(\frac{\partial P}{\partial V}\right)_T = 0. \tag{14}$$

The Diffusion Coefficients

Two approaches are used to describe the diffusion in the liquids: Fick's law and Maxwell–Stefan (MS) theory. The following expression covers the mutual diffusion in binary mixtures:

$$D_{ij} = \Delta \times \Gamma, \tag{15}$$

Δ is the matrix of phenomenological diffusion coefficients and Γ is the thermodynamic factor [1]. Furthermore, the Maxwell–Stefan (MS) [42] diffusion coefficients $Đ_{ij}$ are related to the inverse of the phenomenological diffusion coefficient Δ^{-1} matrix by the relation: $\Delta^{-1} = Đ_{ij}$. In Eq. (15), the phenomenological diffusion coefficient matrix Δ accounts for hydrodynamics, while the thermodynamic factor Γ explains the thermodynamic features of diffusion. Intermolecular forces determine the activity coefficients as well as the effective diffusion ratio governing hydrodynamics [43]. The hydrodynamics contribution on diffusion could be obtained from the Darken model [44]:

$$Đ_{12} = x_2 D_1^* + x_1 D_2^*. \tag{16}$$

The self-diffusion coefficient D^* explains the motion of molecules in a mixture without a chemical potential gradient. The Darken model is highly impactful to predict mutual diffusion in the binary systems [45–47]. The equation of Wilke and Chang [48] was employed to calculate the self-diffusion coefficient D^* as follows:

$$D^* = \frac{7.4\times 10^{-8}(\psi M)^{0.5}T}{\eta \times V^{0.6}}, \tag{17}$$

ψ is the association parameter, M is the molecular weight, and η is viscosity. In the above equation, the association parameter was implemented to define the influence of the solvent molecular weight on the diffusion process. This parameter has a value of 1.0 for unassociated organic solvents. Moreover, mutual diffusion coefficient strongly depends on the non-ideality of the mixture and the thermodynamic factor:

$$\Gamma = 1 + x_i\left(\frac{\partial \ln \gamma_i}{\partial x_i}\right), \tag{18}$$

γ_i stands for the activity coefficient of component i in the mixture. The Γ values were calculated regarding the COSMO-RS model [49] and the COSMOthermX program [50] was applied for COSMO-RS calculations.

RESULTS AND DISCUSSION

Experimental densities were measured by the SVM 3000 Stabinger viscometer and reported in Table 1. Critical properties of pure materials and acentric factors were taken from [51]. Figure 1 shows the changes of the second virial coefficient with temperature obtained from the PRSV equation of state for three binary mixtures. In this figure, the effect of increasing the alcohol chain length on the second virial coefficient is observed. For the benzene + 2-propanol binary system, the second viral coefficient changes from negative to positive at $T = 1267$ K. For the benzene + 2-butanol mixture, the changing temperature reaches to $T = 1315$ K. For the binary mixtures benzene + 2-pentanol, this temperature is 1413 K. The findings indicate that at a constant temperature, as the length of the alcohol in the binary mixtures increases, the amount of attractive interactions increases. The behavior means that the alcohol with the longer chain is more likely to intend with benzene. For the above binary mixtures, third virial coefficients as a function of temperature are presented in Fig. 2. In all cases, this coefficient is negative at low temperatures (below than $T \approx 100$ K), then increases to a maximum (passes through a peak) and decreases gradually. Third virial coefficients for benzene + 2-propanol is maximum, indicating that repulsive forces are more influential in this mixture, and reducing the alcohol length makes more attractive forces. The addition of benzene to the longer chain alcohols reinforces the strength of intermolecular interactions.

Furthermore, the PRSV was used to calculate the Joule–Thomson inversion curve (JTIC) of the mentioned binary mixtures. JTIC separates regions for which heating and cooling occur upon an isenthalpic expansion. Temperature and pressure at which the Joule–Thomson coefficient becomes zero are called the Joule–Thomson inversion point. The region with JTIC > 0 is called the cooling region, while JTIC < 0 is called the heating region. Repulsive forces are dominant at short distances, but attractive forces have the dominant effect at long distances. At high pressures, intermolecular distances among molecules reduce, and repulsive forces are predominant, while at low pressures, attractive molecular forces are more important. The JTIC diagram for binary mixtures is shown in Fig. 3. The peak height in the high-pressure and low temperature range (where attractive forces are dominant) is as follows: benzene + 2-pentanol > benzene + 2-butanol > benzene + 2-propanol. This behavior indicates that in the benzene + 2-pentanol system, attractive forces are more dominant. In the low pressure and high temperature range, (where the repulsive forces are dominant) the maximum point for binary mixtures is as follows: benzene + 2-propanol > benzene + 2-butanol > benzene + 2-pentanol. The behavior indicates that the repulsive forces are larger in the lower chain alcohols.

Table 1. Densities (ρ, g cm^{-3}) the binary mixtures of benzene with 2-alkanol at $p = 0.1$ MPa and different temperatures

x_1	293.15 K	303.15 K	313.15 K	323.15 K
Benzene (1) + 2-propanol (2)				
0	0.7854	0.7768	0.7680	0.7588
0.0881	0.7940	0.7849	0.7759	0.7663
0.1663	0.8015	0.7921	0.7828	0.7730
0.2484	0.8093	0.7996	0.7899	0.7799
0.3532	0.8191	0.8091	0.7992	0.7890
0.4471	0.8279	0.8176	0.8075	0.7971
0.5623	0.8385	0.8281	0.8177	0.8072
0.6592	0.8475	0.8368	0.8263	0.8158
0.7336	0.8543	0.8435	0.8330	0.8223
0.8541	0.8654	0.8546	0.8440	0.8332
0.9317	0.8726	0.8616	0.8509	0.8402
1	0.8787	0.8680	0.8573	0.8466
Benzene (1) + 2-butanol (2)				
0	0.8067	0.7984	0.7898	0.7806
0.0823	0.8112	0.8024	0.7933	0.7843
0.1534	0.8154	0.8063	0.7969	0.7876
0.2332	0.8202	0.8108	0.8013	0.7918
0.3469	0.8273	0.8178	0.8081	0.7982
0.4452	0.8340	0.8243	0.8143	0.8041
0.5514	0.8416	0.8315	0.8214	0.8111
0.6468	0.8488	0.8384	0.8281	0.8179
0.7319	0.8555	0.8449	0.8345	0.8242
0.8533	0.8655	0.8549	0.8442	0.8338
0.9322	0.8726	0.8617	0.8510	0.8407
1	0.8787	0.8680	0.8573	0.8466
Benzene (1) + 2-pentanol (2)				
0	0.8093	0.8012	0.7927	0.7840
0.0764	0.8128	0.8043	0.7954	0.7861
0.1617	0.8169	0.8081	0.7989	0.7895
0.2351	0.8207	0.8117	0.8023	0.7929
0.3463	0.8266	0.8173	0.8078	0.7982
0.4364	0.8320	0.8225	0.8129	0.8032
0.5616	0.8403	0.8305	0.8206	0.8107
0.6541	0.8471	0.8369	0.8268	0.8166
0.7337	0.8534	0.8430	0.8325	0.8222
0.8518	0.8638	0.8529	0.8420	0.8312
0.9341	0.8717	0.8607	0.8498	0.8387
1	0.8787	0.8680	0.8573	0.8466

Standard uncertainties are $u(T) = 0.02$ K, $u(x) = 0.001$, $u(p) = 10$ kPa, expanded uncertainty for density is $U(\rho) = 0.002$ g cm^{-3} (0.95 level of confidence).

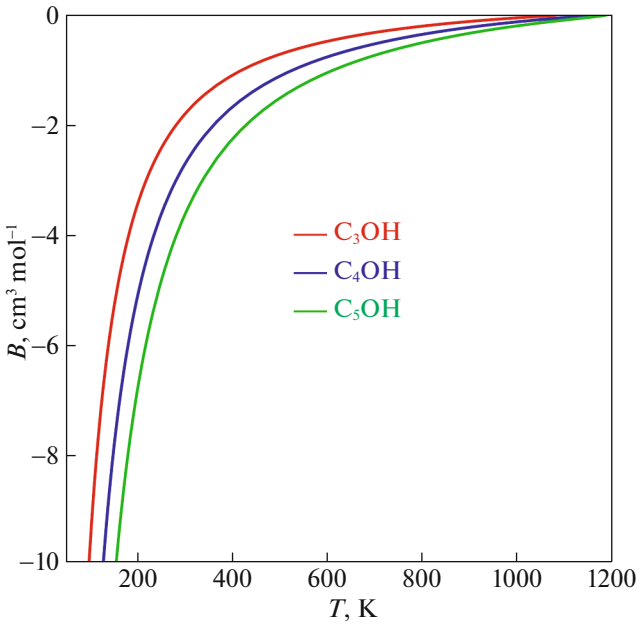

Fig. 1. Second virial coefficient for binary mixtures of benzene (1) + 2-alkanol (2).

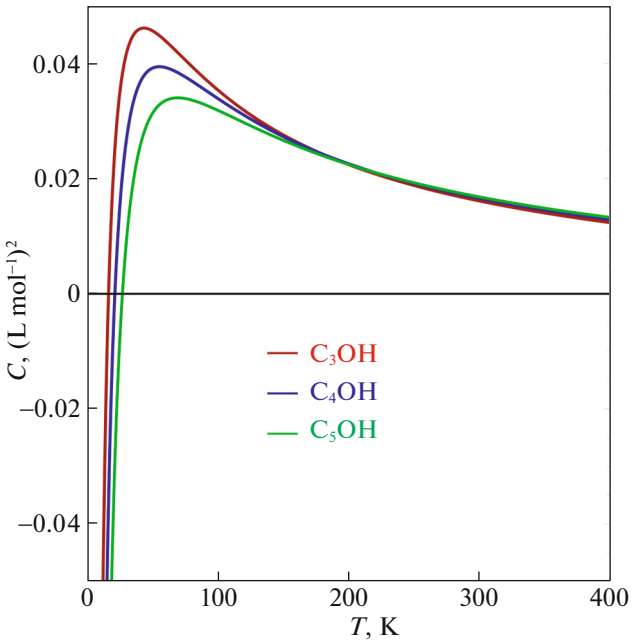

Fig. 2. Third virial coefficient for binary mixtures of benzene (1) + 2-alkanol (2).

Values of thermodynamic factor Γ and mutual diffusion D_{ij} for all systems at $T = 303.15$ K are plotted in Figs. 4 and 5, respectively. The maximum diffusion occurs in the binary mixtures of benzene + 2-propanol, and increasing the alcohol chain reduces the diffusion coefficients. Diffusion in solutions is a function of molecular mass and shape, temperature, mobility, and solute-solvent interactions. For the binary mixtures, the slower movement of benzene in 2-pentanol can be explained by the greater attractive forces among the benzene and 2-pentanol molecules. In fact, benzene molecules are drawn through the attractive forces of longer alcohols. Also, presence of steric hindrances produces by the longer alkyl chain makes benzene diffuse less freely. Furthermore, weaker attractive interactions among unlike molecules in the benzene + 2-propanol mixture, increases the benzene mobility and diffusion process. A literature survey shows that similar behavior is observed for the diffusion of benzene in 1-alkanol, and the alkyl chain of alcohol has a profound effect on lowering the diffusion speed [52].

The thermodynamic factor Γ, which describes the deviation of mixtures from ideal behavior, is crucial because it connects the Fick diffusion coefficient (mutual diffusion or D_{ij}) with the Maxwell–Stefan diffusion coefficient ($Đ_{ij}$). This parameter was calculated for three binary mixtures regarding the COSMO-RS theory. It indicates that all binary mixtures have a positive deviation from ideal behavior, and the molecular forces are weak. The observed behavior in the mixtures suggests that the strength of the interaction between benzene and alcohol molecules follows the order: 2-pentanol > 2-butanol > 2-propanol. In all cases, the alcohol chain plays a central role and reinforces the strength of the interaction between unlike molecules.

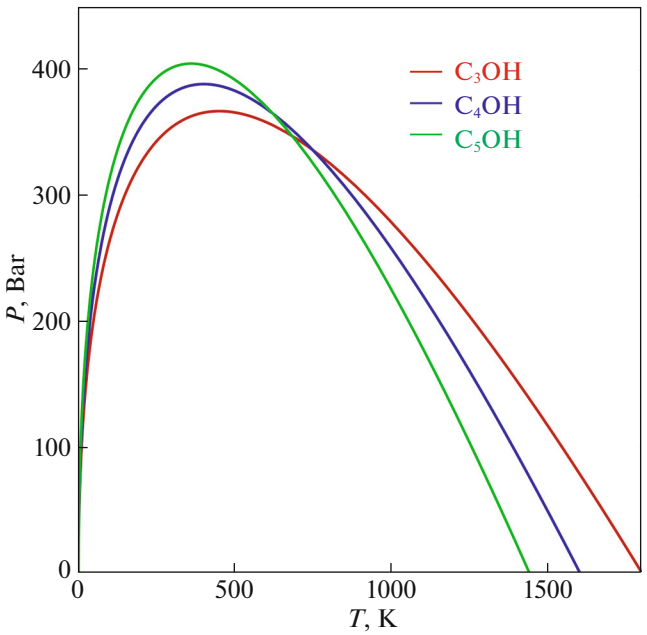

Fig. 3. Joule–Thomson inversion curve for binary mixtures of benzene (1) + 2-alkanol (2).

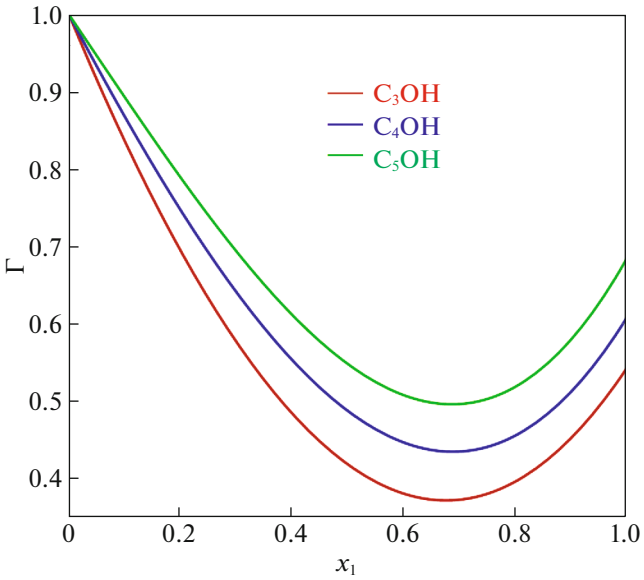

Fig. 4. Thermodynamic factor for binary mixtures of benzene (1) + 2-alkanol (2) at $T = 303.15$ K.

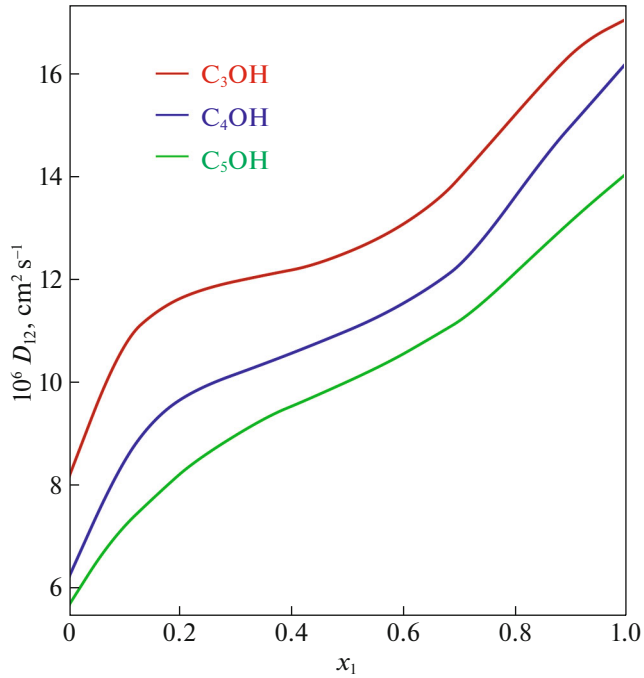

Fig. 5. Mutual diffusion coefficients for benzene (1) + 2-alkanol (2) at $T = 303.15$ K.

CONCLUSIONS

In the current study, to collect information about the effect of the alkyl chain of alcohol on the molecular interaction in the binary mixtures of benzene and 2-alkanol (2-propanol up to 2-pentanol), some parameters namely second and third virial coefficients, the Joule-Thomson inversion curve, the thermodynamic factor, and the mutual diffusion D_{ij} were calculated. The influence of the alkyl chain of the alcohol on parameters mentioned above was discussed. Obtained results show that the longer alcohol chain increases the strength of molecular interactions in the binary mixtures.

ACKNOWLEDGMENTS

The author gratefully acknowledge from Malayer University for financial support.

CONFLICT OF INTEREST

The authors declare that they have no conflicts of interest.

REFERENCES

1. D. A. McQuarrie and J. D. Simon, *Physical Chemistry, a Molecular Approach* (Univ. Science Books, Sausalito, CA, 1997).
2. J. H. Dymond and E. B. Smith, *The Virial Coefficients of Pure Gases and Mixtures: A Critical Compilation* (Clarendon, Oxford, UK, 1980).
3. L. G. Haar, *NIST Standard Reference Database 10-NBS/NRC Steam Tables* (Hemisphere, New York, 1985).
4. C. Tsonopoulos, AIChE J. **20**, 263 (1974).
5. L. Meng, Y. Y. Duan, and L. Li, Fluid Phase Equilib. **226**, 109 (2004).
6. G. Coccia, G. D. Nicola, S. Tomassetti, et al., Fluid Phase Equilib. **493**, 36 (2019).
7. M. J. Assael, J. P. M. Trusler, and T. F. Tsolakis, *An Introduction to Their Prediction Thermophysical Properties of Fluids* (Imperial College Press, London, UK, 1996).
8. G. Di Nicola, G. Coccia, M. Pierantozzi, and M. Falone, Int. J. Refriger. **68**, 242 (2016).
9. B. A. Mamedov and E. Somuncu, Phys. A (Amsterdam, Neth.) **420**, 246 (2015).
10. U. K. Deiters and K. M. de Reuck, Pure Appl. Chem. **69**, 1237 (1997).
11. K. Juris and L. A. Wenzel, AIChE J. **18**, 684 (1972).
12. G. W. Dilay and R. A. Heidemann, Ind. Eng. Chem. Fund. **25**, 152 (1986).
13. B. Haghighi, M. R. Laee, and N. S. Matin, Cryogenics **43**, 393 (2003).
14. P. Proust and J. H. Vera, Can. J. Chem. Eng. **67**, 170 (1989).
15. M. Almasi, Fluid Phase Equilib. **489**, 1 (2019).
16. S. Heydarian, M. Almasi, and Z. Saadati, J. Mol. Liq. **275**, 122 (2019).
17. M. Almasi and R. Daneshi, J. Chem. Eng. Data **63**, 3881 (2018).
18. M. Almasi, J. Chem. Eng. Data **60**, 714 (2015).
19. M. Almasi, Phys. B (Amsterdam, Neth.) **412**, 100 (2013).
20. M. Almasi and H. Iloukhani, J. Chem. Eng. Data **55**, 3918 (2010).

21. M. Almasi and P. Monjezi, J. Chem. Eng. Data **61**, 2510 (2016).
22. H. Iloukhani and M. Almasi, J. Solution Chem. **40**, 284 (2011).
23. M. Almasi, Chem. Phys. **527**, 110474 (2019).
24. Z. Khedri, M. Almasi, and A. Maleki, J. Mol. Liq. **296**, 111767 (2019).
25. S. Ahmadi and M. Almasi, J. Chem. Thermodyn. **142**, 106025 (2020).
26. S. Ebadi and M. Almasi, J. Mol. Liq. **304**, 112792 (2020).
27. M. Almasi, J. Mol. Struct. **1219**, 128576 (2020).
28. B. Sarkoohaki, M. Almasi, and M. Karimkhani, J. Chem. Eng. Data **63**, 2257 (2018).
29. S. Heydarian, M. Almasi, and Z. Saadati, J. Chem. Thermodyn. **135**, 345 (2019).
30. M. Almasi, J. Mol. Liq. **209**, 346 (2015).
31. M. Almasi, J. Chem. Eng. Data **57**, 2992 (2012).
32. M. Almasi, Thermochim. Acta **591**, 75 (2014).
33. Z. Khedri, M. Almasi, and A. Maleki, Chem. Eng. Data **64**, 4465 (2019).
34. M. Almasi and H. Nasim, J. Chem. Thermodyn. **89**, 1 (2015).
35. M. Almasi, J. Chem. Eng. Data **65**, 4498 (2020).
36. M. Almasi and M. Shojabakhtiar, Thermochim. Acta **523**, 105 (2011).
37. M. Almasi, J. Chem. Eng. Data **59**, 275 (2014).
38. M. Almasi and L. Mosuavi, J. Mol. Liq. **163**, 45 (2011).
39. M. Almasi, J. Chem. Thermodyn. **69**, 101 (2014).
40. R. Stryjek and J. H. Ver, Can. J. Chem. Eng. **64**, 323 (1986).
41. I. Polishuk, Ind. Eng. Chem. Res. **48**, 10708 (2009).
42. R. Krishna and J. A. Wesselingh, Chem. Eng. Sci. **52**, 861 (1997).
43. G. Guevara-Carrion, T. Janzen, Y. M. Muñoz-Muñoz, and J. Vrabec, J. Chem. Phys. **149**, 064504 (2018).
44. X. Liu, T. J. H. Vlugt, and A. Bardow, Ind. Eng. Chem. Res. **50**, 10350 (2011).
45. C. D'Agostino, M. D. Mantle, L. F. Gladden, and G. D. Moggridge, Chem. Eng. Sci. **66**, 3898 (2011).
46. G. D. Moggridge, Chem. Eng. Sci. **76**, 199 (2012).
47. G. D. Moggridge, Chem. Eng. Sci. **71**, 226 (2012).
48. C. R. Wilke, Pin Chang, AIChE J. **1**, 264 (1955).
49. A. Klamt and F. Eckert, Fluid Phase Equilib. **172**, 43 (2000).
50. *COSMOthermX Program* (Cosmologic, Leverkusen, Germany, 2018).
51. C. L. Yaws, *Yaws Handbook of Thermodynamic and Physical Properties of Chemical Compounds* (William Andrew, 2008).
52. J. Winkelmann, *Diffusion in Gases, Liquids, and Electrolytes, Landolt–Bornstein: Numerical Data and Functional Relationships in Science and Technology* (Springer, New York, 2018).